Environmental Technology & Innovation 33 (2024) 103494

Contents lists available at ScienceDirect

Environmental Technology & Innovation

journal homepage: www.elsevier.com/locate/eti

# Influence of hydrodynamic shear stress on activated algae granulation process for wastewater treatment

Ngoc-Kim-Qui Nguyen [a,b], Xuan-Thanh Bui [a,b,*], Thanh-Son Dao [a,b], Mai-Duy-Thong Pham [a,b], Huu Hao Ngo [c], Chitsan Lin [d], Kun-Yi Andrew Lin [e], Phuoc-Dan Nguyen [a,b], Ky-Phuong-Ha Huynh [a,b], Thi-Kim-Quyen Vo [f], Van-Tung Tra [g], Thanh-Son Le [b,h]

[a] Ho Chi Minh City University of Technology (HCMUT), 268 Ly Thuong Kiet Street, District 10, Ho Chi Minh City, Viet Nam
[b] Vietnam National University Ho Chi Minh City (VNU-HCM), Linh Trung ward, Ho Chi Minh City 700000, Viet Nam
[c] School of Civil and Environmental Engineering, University of Technology Sydney, Sydney, NWS 2007, Australia
[d] Department of Marine Environmental Engineering, National Kaohsiung University of Science and Technology, Kaohsiung City, Taiwan
[e] Institute of Analytical and Environmental Sciences, National Tsing Hua University, Hsinchu, Taiwan
[f] Ho Chi Minh City University of Industry and Trade (HUIT), 140 Le Trong Tan street, Tay Thanh ward, Tan Phu district, Ho Chi Minh City, Viet Nam
[g] Institute of Applied Technology and Sustainable Development, Nguyen Tat Thanh University, Viet Nam
[h] Institute for Environment and Resources, 142 To Hien Thanh street, district 10, Ho Chi Minh City, Viet Nam

ARTICLE INFO

*Keywords:*
Shear stress
Granulation
Activated algae
Microalgae
Filamentous cyanobacteria

ABSTRACT

In this study, activated algae granule was formed by cultivating a mixed culture of the microalga *Chlorella vulgaris* and activated sludge in batch photobioreactors (PBRs). Without aeration, the granulation process was investigated through four different agitation speeds of 80, 120, 160, 200 rpm (shear stress of 0.04, 0.15, 0.35, 0.69 Pa). Hydrodynamic shear stress created by agitation affected the activated algae granulation through microeddies. The largest granule was achieved in the PBR with agitation speed of 200 rpm (R200) with shear stress of 0.69 Pa (size of 339 μm). In the other hand, lower shear stress in R160 (shear stress of 0.35 Pa) gave optimal results in terms of wastewater treatment efficiency and granule formation time (165 days of operation). Shear stress below 0.15 Pa (120 rpm) showed no granule formation during 220 days operation. While shear stress from 0.04–0.15 Pa could guarantee mass transfer for the entire co-culture without aeration, shear stress from 0.15–0.69 Pa was a suitable range for the granulation process of activated algae. This study reveals that activated algae granule formation through agitation mechanism is a promissing solution for wastewater treatment and microalgae biomass recovery to substantially increase the share of renewable energy in the global energy mix.

## 1. Introduction

In the early 1950s, the utilization of microalgae for the wastewater treatment was firstly reported by Oswald et al. (1957). Until

* Corresponding author at: Ho Chi Minh City University of Technology (HCMUT), 268 Ly Thuong Kiet Street, District 10, Ho Chi Minh City, Viet Nam.
*E-mail address:* bxthanh@hcmut.edu.vn (X.-T. Bui).

https://doi.org/10.1016/j.eti.2023.103494
Received 17 November 2023; Received in revised form 16 December 2023; Accepted 17 December 2023
Available online 20 December 2023

1970s, the term "activated algae" in wastewater treatment field was raised referring to the symbiotic combination between microalgae and bacteria (McGriff and McKinney, 1972). In the co – culture system, microalgae play a role in consuming ammonium ($NH_4$) in wastewater and $CO_2$ in the atmosphere to synthesize organic molecules and release oxygen ($O_2$). Meanwhile, bacteria from activated sludge (AS) will consume $O_2$ which provided from microalgae to decompose organic matter and release carbon dioxide ($CO_2$) for microalgae activities (Oswald et al., 1957; Spolaore et al., 2006). With this symbiotic cycle, wastewater treatment system coupled with activated algae (AA) could reduce 75% of total cost by the aeration elimination (Åmand et al., 2013). Besides that, the bacteria-microalgae consortia system can treat wastewater with 15% higher efficiency than pure microalgae wastewater treatment and has shorter processing time, and the recovered biomass can be used for many different purposes such as biofuels, biofertilizers, animal feed, and biochemical products (Lisa Aditya et al., 2022). Therefore, it can be said that wastewater treatment based on activated algae is Green Technology for Sustainable Water (Bui et al., 2021).

Numerous studies have demonstrated the feasible utilization of AA as an environmental-friendly wastewater treatment method (Wang et al., 2010) because of its remarkable performance in treating many types of wastewaters including piggery (Ji et al., 2013; Zheng et al., 2019), industrial (Muñoz et al., 2009), domestic wastewater (Dang et al., 2023), transforming waste into valuable materials.

With fast-growing capacity and valuable pigments production such as fucoxanthin, lutein, β-carotene (von Alvensleben et al., 2016), rather than wastewater treatment, microalgae can also be employed in a lot of industrial applications including nutraceuticals, pharmaceuticals, and aquafeed (Ifland et al., 2015; Kaur, 2020). Some of the most prevalent techniques for algal biomass harvesting are centrifugation, filtration, flotation and flocculation. Recently, ceramic microfiltration membrane is proven its ability on microalgae solution enrichment and harvesting (Lisa Aditya et al., 2023). One of the commonly used methods is to use chemical flocculation such as cationic polyacrylamide flocculant (Nguyen et al., 2019). To recover *Chlorella vulgaris* biomass, cationic polyacrylamide at the dose of 36 mg/g dry weight was used (Vu et al., 2020). These technologies are facing to many drawbacks, especially the high cost, which consume 20–30% operating cost during microalgae cultivation (Renuka et al., 2013). Recently, flocculation of microalgae and bacteria which developed through cell self-aggregation is a potential strategy for wastewater treatment coupling with biomass recovery. Although flocculation of algal biomass was indicated to have a good settle ability of 0.05 g $l^{-1}$ $min^{-1}$, this rate was still slower than AS, 0.07 g $l^{-1}$ $min^{-1}$ (Su et al., 2012). Therefore, the compact structure and high biomass density of AA granule is predicted not only contain all the advantages from microalgae and AS as mentioned above, but also shows economic efficiency when it can settle quickly due to its gravity without any added chemicals. In addition, wastewater treatment with AA can be coupled with other technologies such as sponge membrane bioreactor to treat wastewater with high salinity and organic content (Vo et al., 2021) or coupled with MBR processes to treat wastewater microplastics (Bui et al., 2020) and nutrient recovery (Vu et al., 2022).

Operational stresses are among the major factors determining the granulation capacity of the microbial community. For the susceptibility of microorganisms, stress can be caused by various factors such as temperature, light intensity or nutrition supplement for microorganisms (Zhou et al., 2015; Liu et al., 2016; Meng et al., 2019). A type of hydrodynamic stress generated from mixing is shear stress, a critical factor requiring careful consideration in granulation process at different scales. Without aeration, mixing is a sustainable alternative to maintain homogeneity of high cell density inside the reactor, overcome limitation and diffusion gradients. However, microalgal species react differently to mixing because each species has its own optimum mixing, necessitating the use of a unique mixing and culture apparatus (Leupold et al., 2013). It was confirmed that significant shear stress would lead to increase the cohesion of the microalgae, allowing them to grow faster hence more biomass (Fanesi et al., 2021). In the granulation of AA, shear stress was a challenging operation condition, and a stable value should be found where the mixing is sufficient for optimal cell growth without compromising its integrity. Previous studies showed that the agitation speed in the range of 100 – 200 rpm is applied for major experiments to create a successful AAG with the size reaching 0.6 – 4.5 mm (Tiron et al., 2015; Milferstedt et al., 2017; He et al., 2018; Abouhend el al, 2018; Ansari et al., 2019; Bumbac et al., 2019; Ahmad et al., 2019) (see E-supplementary (Table S1)). However, the optimal AAG particle size to achieve the best wastewater organic treatment is reported to be in the range of 1.2 – 1.3 mm (Ji et al., 2022). Therefore, maintaining the AAG size is one of the important goals in applying the AAG process wherein finding the suitable agitation condition is one of the key factors to ensure this works. Moreover, a superficial stirring speed of around 140 rpm in the cylindrical reactor showed that not only improved photosynthetic efficiency, biomass productivity, specific growth rate, average pore size, and microalgae-to-bacteria ratio of AAG but also accelerated pollutants removal for AAG process wherein organics removal significantly correlated with stirring (Shen et al., 2023). Therefore, the agitation speeds in the range of 80 – 200 was chosen to investigate. Hydrodynamic shear in turbulent flow is explained by eddies whose energy content scales downward with their size. In the granulation process of activated sludge, low energy intensity of eddies with smaller size than particles made their effects on these particles is negligible. Eddies with equal or slightly smaller size than particles can transmit turbulent forces - including shear force - to these cells, while the larger ones would simply entrain them convectively (Henzler, 2000; García Camacho et al., 2001). However, the specific range of smaller and larger size of eddies compared to particles in the granulation of AA using agitation has not been discovered yet. Therefore, this study aims to investigate the effects of the shear stress or agitation speeds on i) granulation of activated algae and ii) their wastewater treatment performance.

## 2. Materials and methods

### 2.1. Microbial sources and synthetic wastewater

The microalga *Chlorella vulgaris* was used as biological inoculum for granulation processes in this study was taken from Aquaculture Research Institute 2, Ho Chi Minh City, Vietnam. AS taken from a membrane bioreactor was pretreated by settled down for 3 h to

remove suspended solids, then centrifuged for 10 min at 3600 rpm. Before utilized as a source of bacterial consortium, the settling solids were washed twice with distilled water. The initial mixed liquor suspended solids (MLSS) of the co-culture was 600 mg/L with microalgae: activated sludge ratio of 5:1 (dry weight) (Su et al., 2012).

This study used synthetic wastewater with C:N:P mass ratio was 100:10:1 for the sufficient nutrient and organic source during granulation process based on previous studies of Tiron et al., (2015, 2017). Synthetic wastewater composition was prepared with distilled water and macroelements according to Huang et al. (2015), with minor modification including 187.44 g $L^{-1}$ glucose; 256.41 g $L^{-1}$ sodium acetate; 152.86 g $L^{-1}$ $NH_4Cl$; 43.88 g $L^{-1}$ $KH_2PO_4$; 27.75 g $L^{-1}$ $CaCl_2$; 51.35 g $L^{-1}$ $MgSO_4.7\ H_2O$; 24.83 g $L^{-1}$ $FeSO_4.7\ H_2O$. Trace element solution composition was followed the detailed information in Nguyen et al. (2016) Vo et al. (2018).

### 2.2. Experimental design

Co-culture of microalgae and AS was represented by granulation developed in 4 stirred photo-bioreactors (PBRs) with 7 L working volume containers (H x D = 42 cm × 17 cm). The PBRs were continuously illuminated with a light intensity of 3800 – 4000 lux white LED lights (SMD 5050), and a light:dark cycle of 12:12 (h). The constant agitation of each reactor was implemented by a stirring shaft with two propellers (2.7 cm in diameter and 34 cm in length) placed on the top. The PBR system was installed in a wooden box with a thickness of 10 mm to prevent light loss and temperature fluctuation (maintained around 27–32 °C).

The pH of fed wastewater was controlled between 7.0–7.5 by $NaHCO_3$. The granulation process was performed in sequencing batch mode, volume exchange ratio of 50%, at four different agitation speeds of 80, 120, 160, 200 rpm, corresponding to 4 different shear stress values. Overtime changing in batch cycle operation was described in E-supplementary (Table S2). At the beginning of acclimatization period, a batch cycle comprised 3 days operation because of the low initial seed biomass, compared to the pollutants' concentration in feeding wastewater. Due to the small size and low density of the seed biomass, the settling time was fixed at 3 h to maintain the biomass in the reactor. When microorganisms in the co-culture were more stable, batch cycle was carried out in 48 h. Settling time was also gradually reduced from 3 h to 60, 15 and 5 mins, to increase washout of small biomass during the experiment, which is necessary for granulation. According to the experimental progress, 3 different settling times of 60, 15, 5 mins corresponding to stage 1 (day 28 – 36), stage 2 (day 37 – 106), stage 3 (day 107 – 220) were implemented, respectively. The settling time reduction was determined every time the settle ability reached greater than 95% after 2 consecutive weeks. Settling ability was determined by the following equation:

$$Settling \quad ability = 100 \times (1 - \frac{X_s}{X_m}) \tag{1}$$

Where $X_m$ is the well-mixed TSS concentration (mg $L^{-1}$), $X_s$ is the TSS concentration in the effluent (after settling) (mg $L^{-1}$).

### 2.3. Analytical parameters

#### 2.3.1. Physical and chemical characterization

The effluent was withdrawn by an effluent valve, filtered using a filter membrane with a pore size of 0.45 μm (Fisher Whatman puradisc-25 mm) and stored in Erlenmeyer flask for analysis within 1 h after sampling. Water quality parameters (chemical oxygen demand – COD, total phosphorous – TP, total suspended solids – TSS, $NH_4^+$-N, $NO_3^-$-N, $NO_2^-$N) were analyzed according to standard methods (APHA, 2005). The dissolved oxygen (DO) concentrations and pH were measured by probes (Hanna HI 9146, Hanna HI 9813–6, Italia). Light intensity was measured using a light sensor (US-SQS/L, ULM-500, FA Walz, Germany).

#### 2.3.2. Biomass characteristics and microscopic observation

The biomass sample was measured as MLSS (APHA, 2017). Microscopic observation was examined by light micrscope (OPTIKA B-150). Particle size distribution (PSD) analysis of mixed liquor samples was performed using a Laser Scattering Particle Analyzer (HORIBA LA-920, Japan) and processed data by WET(LA-920) Ver.3.37 system for Windows. The measured particle size was ranged from 0.51 to 2000 μm.

#### 2.3.3. Microbial parameters

To represent microalgae biomass growth, chlorophyll-a (Chl-a) concentration in mixture of AS and microalgae was analyzed using acetone as an extract solution (Dang et al., 2018). Briefly, 20 mL of the well-mixed sample from each PBR was centrifuged at 4000 rpm for 10 min. The supernatant was discarded, and the residual was resuspended with 20 mL of 90% acetone solution and 0.05 g $CaCO_3$ and then being sheared by a vortex mixer for 1 min. The top suspension was stored at 4 °C for 24 h in darkness. Finally, the suspension was centrifuged at 4000 rpm for 10 min to remove any suspended solids from the supernatant before the Chl-a determination. The Chl-a concentration was measured at 6 different wavelengths of 630, 645, 663, 750, 772 and 850 nm by ultraviolet spectrophotometry. The 90% acetone solution was used as the blank. The Chl-a calculation was performed following the below equations:

**Total *chlorophyll-a* concentration ($c_t$, μg $L^{-1}$)**

$$c_t = \frac{[11.64(OD_{663} - OD_{750}) - 2.16(oD_{645} - OD_{750}) + 0.10(OD_{630} - OD_{750})]V_1}{V.\sigma} \tag{3}$$

Where V is the volume of each sample (L), and $V_1$ is the volume of acetone-based extract (mL). OD is the absorbency at corresponding

wavelength and σ is optical path of cuvette (cm).

***Chlorophyll-a* of photosynthetic bacteria ($c_b$, μg $L^{-1}$)**

$$c_b = \frac{[25.2(OD_{772} - OD_{850})]V_1}{V.\sigma} \quad (4)$$

***Chlorophyll-a* of algae (c, μg $L^{-1}$)**

$$c = c_t - c_b = \frac{[11.64(OD_{663} - OD_{750}) - 2.16(oD_{645} - OD_{750}) + 0.10(OD_{630} - OD_{750}) - 25.2(OD_{6772} - OD_{850})]V_1}{V.\sigma} \quad (5)$$

***Extracellular polymeric scubstances*.**

Extracellular polymeric substances (EPS) play a crucial role in building and maintaining structural integrity of aerobic granules through cohesion and adhesion of microbial cells (Liu et al., 2005). The EPS can be classified into bound EPS (inside granule) and soluble EPS (dissolved in bulk liquid), and only soluble EPS would be biodegradable (Laspidou and Rittmann 2002). The analysis procedure of bound EPS was done through four steps: i) 50 mL of well mixed biomass in centrifugal tube was centrifuged at 4000 rpm for 20 min, ii) The supernatant was discarded, the tube with residue solid biomass which contain bound EPS then was filled to 50 mL by NaCl 0.9%. The supernatant removed from this step then be used for soluble EPS analysis. NaCl was used as a solvent to extract bound EPS from granule. Then iii) the fulfilled tube was heated at 80 °C in 1 h, then cooled at room temperature before iv) centrifuged again at 4000 rpm, 20 min to separate bound EPS and granule. The supernatant solution, which was now containing bound EPS, then be analyzed for PS and PN concentration, using the methods of Dubois et al. (1956) and Lowry et al. (1951). Two types of EPS were determined in term of polysaccharides (PS) and protein (PN) per milligram of TSS.

### 2.3.4. Shear stress

In the PBR system, related to particle settling theory, turbulent flow occurs when the Reynolds number is greater than 2000 (Metcalf and Eddy, 2014). Flow is in transitional condition when Reynolds ranging from 1–2000 and in laminar flow when lower than 1. In this study, the agitation speeds all creating a turbulence environment. Power number for impeller depends on blade characteristics (not liquid viscosity). In addition, the scale or size of an impeller and the elevation of the impeller above the tank bottom has a very small effect on its power number. In this study, two impellers were used on the same shaft with the ratio of distance between two impeller (S) over diameter of impeller (D): S/D = 4, a combined power number of two impeller was calculated to be approximately 166% compared to single-impeller power. Therefore, the power number of two impellers in this study was chosen $K_{combined} = 0.5644$ (Jirout and Rieger, 2011).

Four PBRs with different agitation speeds of 80, 120, 160, 200 rpm were designated as R80, R120, R160, R200, with the relevant shear stress of 0.04, 0.15, 0.35, 0.69 Pa, respectively. Mathematical equations of the stirred PBR for hydrodynamic parameters and detailed value for shear stress calculation were described in the E-supplementary (Table S3, S4).

## 2.4. Statistical analyses

All statistical analyses were performed using the package IBM SPSS Statistics software 20. Parametric one-way analysis of variance (ANOVA) was used to examine significant differences among groups of samples and to obtain the regression analysis. The significance of the ANOVA model is evidenced by the lesser p-value $< 0.05$, which indicated the significance at 95%.

## 3. Results and discussions

## 3.1. Treatment performance

### 3.1.1. Organic removal

Although there were fluctuations during the whole experiment, mean COD removal efficiency of 4 agitation speeds was ranging from 87.6 – 94.8%. This outperformed study of Xu et al., 2017, where their COD removal efficiency ranged from 78.2 – 80.1% at an initial COD of 200 mg/L. The COD removal efficiency of activated algae under the agitation condition could be from 80–96% in some previous studies (Nguyen et al., 2020; Dang et al., 2022b). These findings have indicated that AA is a potential system for the treatment of organic pollutants even without aeration.

Overtime, experimental progress is divided into 3 stages: stage 1 (day 28 – 36), stage 2 (day 37 – 106), stage 3 (day 107 – 220). At stage 3, activated algae granule (AAG) appeared in all 3 PBRs with medium to high agitation speeds, in order of appearance from before to later, respectively R160, R200, and R120. The one-way ANOVA statistical values showed that the effect of different agitation speeds on the COD treatment capacity of activated algae in both aggregates (stage 1, stage 2) and granules formation (stage 3) was insignificant ($p > 0.05$). Additionally, COD removal capacity increased uniformly in the all of AAG-contained PBRs (R120, R160, R200) and AAG-free PBR (R80) again showed that the formation of AAG, and the different agitation speeds did not have significant influence on the COD removal capacity.

### 3.1.2. Nutrients removal

During 220 days of the experiment, except for some days of initial period, $NO_2^-$-N concentration was always in the negligible value (< 1 mg/L). At stage 1 (day 28 – 36), $NH_4^+$-N removal efficiency of the two PBRs with higher agitation speeds (R160, R200) was

significantly superior to that of the two PBRs with lower agitation speeds (R80, R120). Additionally, effluent concentrations of $NO_2^-$-N and $NO_3^-$-N of the 4 PBRs showed that nitrification was more effective in PBRs with higher agitation speeds in the early stage of the experiment. Specifically, mean $NO_3^-$-N concentrations of R80, R120, R160, R200 during stage 1 were 3.76 ± 3.28, 5.08 ± 4.68, 11.09 ± 4.03, 12.88 ± 4.04 mg/L, respectively. These results suggested that higher agitation speeds may have the potential to replace aeration under the conventional operating conditions of AS to remove $NH_4^+$-N through nitrification process, because shear stress generated by high agitation will increase turbulence for the liquid inside PBRs, thereby reduce the depth of the boundary layer, improving the oxygen transfer throughout the bulk liquid and exposure to the air of bacteria (Baquero et al., 2018).

Through stage 2 (day 37 – 106), the mean $NH_4^+$-N removal efficiency of R120 increased sharply, reaching 86.26% compared to 57.6% in stage 1. The $NH_4^+$-N removal capacity of all 4 PBRs still increased and remained stable in the range of 70.5–93.6% with a distinct partition between 2 higher agitation speeds R160, R200 (92.4–93.6%) and 2 lower agitation speeds R80, R120 (70.5–86.3%). Efficient mixing of the co-culture causes rapid circulation of microalgal cells between the dark and illuminated zones that can increase both the photosynthetic activity and productivity of microalgae, thereby increase nutrients removal ability inside high-agitated reactors (Masojídek et al., 2021). Statistical comparison indicated that the speeds within high or low agitation level had no difference in ammonia nitrogen treatment efficiency ($p > 0.05$).

At the end of stage 3, the total biomass of all 4 PBRs ranged from high to low of 2936 ± 501, 2846.3 ± 426, 2748.2 ± 663, 2464.1 ± 270 mg/L, corresponding to reactor R80, R120, 200, and R160, respectively. Self-shading effects have been reported in the photoautotrophical cultivation of *Chlorella vulgaris* using flat panel airlift when total biomass reached 690 ± 20 mg/L (Benavente-Valdés et al., 2017). Therefore, this value of high biomass increased the likelihood of self-shading effects and attenuation of light distribution, thereby reducing light penetration through the whole co-culture of 4 reactors. Since microalgae grow in dense suspensions of co-culture, sufficient mixing is essential in order to expose cells to light equally (Masojídek et al., 2021). Owing to the turbulent flow in PBRs, microalgal cells are continuously cycled between the irradiated and dark zones in the reactor, which causes highly inhomogeneous light distribution within the PBR (Sfroza et al., 2012). Additionally, total biomass of 4 PBRs was inversly propotional with their $NH_4^+$-N treatment efficiency. From low to high, $NH_4^+$-N treatment efficiency of R80, R120, 200, and R160, was 77.7%, 84.46%, 85.02%, 94.0%, respectively. In other words, high agitation speeds may help the microalgae inside PBRs overcome self-shading phenomena to increase their exposure to light, promoting AA in $NH_4^+$-N uptake.

Besides, the impellers configuration using for agitation could also affect motion of the bulk liquid inside the reactor, which indirectly influenced on the granulation process of AA (Verma et al., 2019). Marine impellers were used in our present study. The enhanced agitation speeds, instead of contributing to the formation of intolerable shear zones for granulation of AA, provided axial motion and of the bulk liquid in the reactor, circulate the liquid towards axis and then raise it along the walls to reduces settling of biomass (Verma et al., 2019). It pointed out that, when there was no aeration, agitation helped ensure mass transfer, water flow, increase dissolved gas from atmosphere into liquid phase and help to transfer the particle throughout the medium (Henzler, 2000; García Camacho et al., 2001). Microalgae thus could contact nutrients and inorganic carbon source ($CO_2$) to grow their biomass.

Although mass transport and microalgal growth will be improved in conditions of higher agitation speed, excessive shear stress could lead to higher detachment thus affecting process stability. Microalgal cells could be damaged by rupturing of the gas bubbles at the culture surface created from mechanical agitation and this damaging effect is dependent on microalgae species (Ajala and Alexander, 2022). Therefore, figure out the suitable range for shear stress in the implementation of AAG for wastewater treatment, coupling with biomass recovery is an important fundamental step for sustainably widespread the utilization of renewable energy from microalgae.

### 3.2. Chlorophyll-a profile

One-way ANOVA statistics showed that different agitation speeds influenced *Chl-a* concentration ($p < 0.05$) while negligibly impacted on total biomass ($p > 0.05$). The pairwise comparisons in the Posthoc comparison showed that, with the same pattern with $NH_4^+$-N and $NO_3^-$-N, *Chl-a* was differed by two subgroups, lower agitation speeds (R80, R120) and higher agitation speeds (R160, R200). Since microalgae are typically grown in suspension in wastewater treatment reactors, complex hydrodynamic conditions can alter environmental factors and affect their physiological properties (Guofang et al., 2020). In other words, shear stress generated by mechanical agitation affected microalgae activity in co-culture, thereby causing changes in AAG's granulation process.

*Chl-a* in microalgae is a commercially important natural green pigment responsible for the absorption of light energy and its conversion into chemical energy via photosynthesis. Among various operating conditions, agitation has been reported to affect chlorophyll content in microalgae (Veronica et al., 2017). From stages 1–3, *Chl-a* concentration at 4 PBRs all increased continuously and reached over 10,000 μg/L at stage 3. Under the granulation stage, if *Chl-a* at R160 and R200 were approximately the same between 10,500 and 11,000 μg/L, *Chl-a* at R120 was 1.5 times higher than this value, up to about 15,000 μg/L. This result indicated one of the well-known responses to stress in microalgae, decrease in photosynthetic pigment contents (e.g. *Chl-a*) upon the increased stress (Pancha et al., 2015). Orderly, AAG was firstly appeared in R160, R200 and R120 (E-supplementary, Fig. S1) on day 165th, day 172nd, and day 188th of operation. This result demonstrated that, if the lower agitation speeds was more favorable for photosynthetic pigments accumulation, it required a longer period of time for AA to get enough shear stress to form AAG.

### 3.3. Correlation between agitation speed, shear stress and tip speed

Shear stress is a function of a fluid's shear rate and viscosity, which continuously imposed on cells in different stages of the life cycle in PBRs. Shear stress level can be represented as critical shear stress (Pa) or critical impeller tip speed (m/s). .

Tip speed was a calculated value based only on the design parameters of the impellers and the agitation speed (See E-Suplementary, Table S2), thus it had a linear relationship with the agitation speed. On the other hand, turbulence, eddy size, and viscosity are the most prominent parameters of shear stress which affect microalgal cells during cultivation (Chinchin Wang, 2018). Therefore, under


**Fig. 1.** Biomass evolution of a) R80, b) R120, c) R160, d) R200.

granulation process, the growth rate of shear stress when increase agitation speed was markedly different from tip speed. Specifically, shear stress only increased with the same angular speed with agitation at lower speed (R80, R120). Stepping through the higher threshold (R160, R200), the rate of shear stress increase will grow rapidly and exceed the linear function. Therefore, to evaluate the role of different agitations on the granulation process of activated algae (microalgae and AS), we chose shear stress as the representative value. In this study, shear stress values have increased with the increase in the impeller agitation speed. R80, R120, R160, and R200 have shear stress of 0.04, 0.15, 0.35, and 0.69 Pa, respectively (See E-Suplementary, Table S2). .

### 3.4. How shear stress from agitation impact on granulation process of AAG

On day 165th, while AAG has appeared in R160, there was no AAG appeared in the lower shear stress of R80 and R120 (0.04 – 0.15 Pa). In our study, PSD was measured when AAG firstly appeared in R160 (Fig. 3a) and right before ending stage 3 (Fig. 3b). From initial 2–10 μm cell size of *Chlorella vulgaris* and 0.5–5 μm size of AS, the mean diameter of AA inside 4 PBRs R80, R120, R160, R200 has developed to 178.71, 179.3, 326.97, 303.53 μm at day 165th (Wu et al., 2009; Wander et al., 2017). At that time, the eddy size inside the lower shear stress reactors was slightly smaller than the AA size, with the size ratio of eddy: AA = 0.54 – 0.9. On the other hand, when entering the higher shear stress threshold from 0.35–0.69 Pa (160 – 200 rpm), eddy size tended to be much smaller than AA with the size ratio of eddy: AA = 0.08 – 0.29. At this point, the tendency of granulation was more dominant in activated algae co-culture with the appearance of AAG in R160. This indicated that the higher shear not only ensured mass transfer conditions, but also assisted the formation of compact and denser granules, shaping the granules into rounded aggregates by removing outgrowing structures, and significantly causing stress on the AA through the small microeddy to form AAG (Britt et al., 2018). This result showed a different effect pathway of hydrodynamic shear stress of agitation on granulation of AA, compared to the granulation of AS in our review. With AS granulation, if eddies with equal or slightly smaller size than particles can transmit shear force to AS cell to form granule (Henzler, 2000; García Camacho et al., 2001), only eddies with much smaller size compared to the AA floc (size ratio of eddy: AA = 0.08 – 0.29) can help appear granulation process on co-culture of AA. Therefore, it could be concluded that with the appearance of microalgae, the higher length scales of shear energy dissipation compared to particle sizes could explain the enhanced granulation in the higher shear stress condition (Joseph et al., 2021).

Till the end of the experiment, except AAG in R200 increased to 339.1 μm, mean particle size of R80, R120, R160 then decreased to 145.98, 160.08, 259.56 μm on day 216th, respectively. While PSD pattern in the PBRs with the lower shear stress (R80, R120) did not show any significant difference over 50 days operation, PSD in the higher ones showed a narrow distribution and appearance of larger AA flocs and AAG inside the reactors. It pointed out that 28 days operation from the day appear AAG in R120 (day 188th operation) to day 216th may not enough for AAG to develop comprehensively. In other words, 50 days is suggested to be the suitable time to figure out the difference in AAG development process. Additionally, this pattern also indicated that at higher agitation speeds of R160, R200, the granulation of AA to form AAG has helped the AA gradually uniform and growing in size.

### 3.5. Shear stress affected on EPS secretion

It is well-established that EPS are important for the granulation and long-term stability of activated granular sludge (AGS). For AA granulation process, EPS content is positively correlated with the self- aggregation property and biomass growth of the isolated microalgal strain under the suitable conditions, which might be one crucial factor for the aggregation of the isolated microalgae and formation of algal-bacterial AGS (Nuramkhaan et al., 2019). Previous work by Tay et al. (2001) indicated that enhanced aeration, which induced higher shear stress on granule, led to increase promotion of PS formation and enhanced granulation process. This was similar to our present study where in the stage 2, when the big flocs of AA were formed, PS was highest in R160 and R200, corresponding to the highest shear stress. From day 75th onward, the number of EPS calculated per unit of biomass tended to decrease gradually due to the growth of total biomass (Fig. 4). Research by Li et al. (2006) confirmed that during granulation process, the longer starvation due to substrate limitations forced microorganisms to use EPS as a substitute for energy source, resulting in a properly controlled EPS concentration to promote granulation. Therefore, this result indicated that microorganisms were in the process of starvation - a phenomenon in which the environment's substrate was not enough to provide for the normal growth of microorganisms.

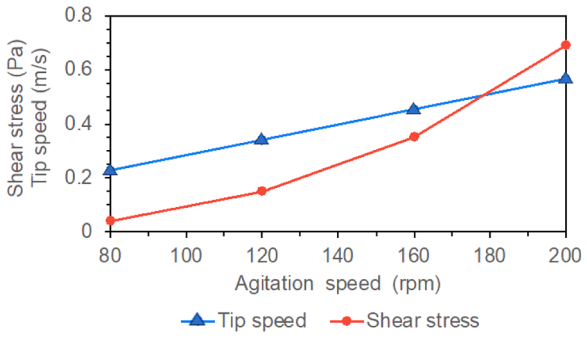


**Fig. 2.** Correlation between agitation speed, shear stress and tip speed.

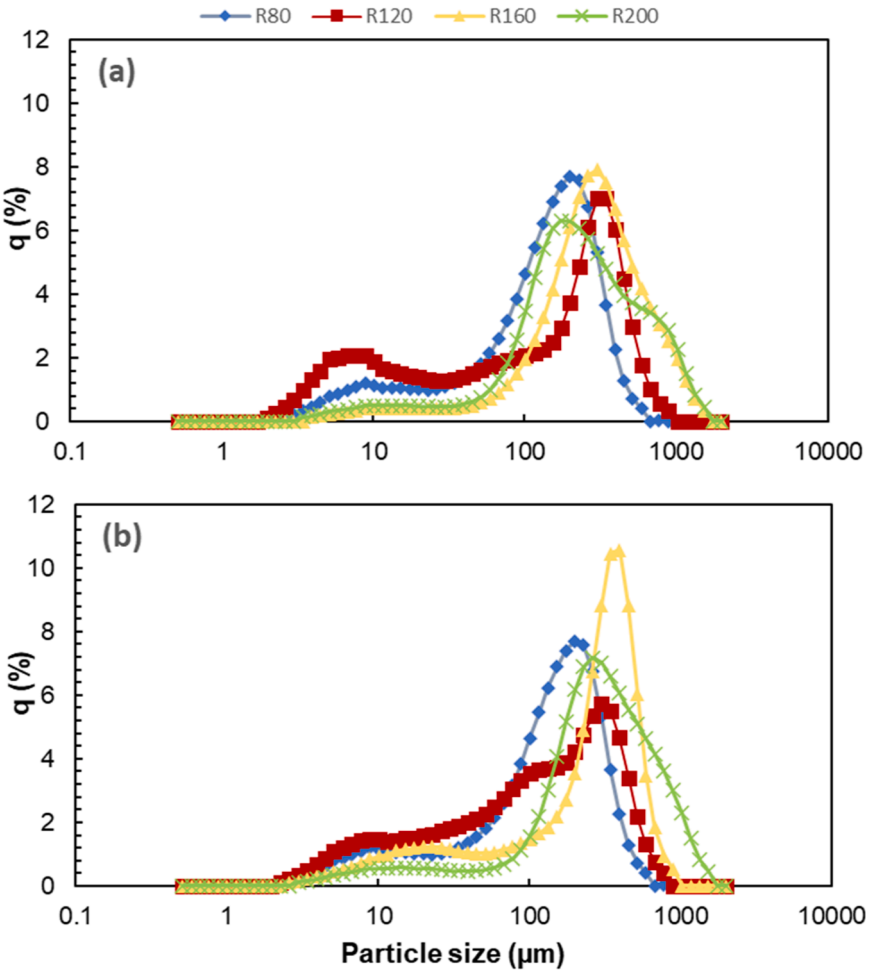


**Fig. 3.** Particle size distribution (PSD) of 4 PBRs in a) on day 165th, b) on day 216th.

Chen et al. (2010) reported that a high PN/PS ratio led to a growth in the hydrophobicity of the floc structure, decrease in surface charge, thereby increased the bonding capacity between flocs to form granule. The higher PN/PS in the outer cell layer facilitates the stability of the sludge structure, while bound EPS containing lower PN/PS might implied that PS contributes more to the stability of the sludge internal structure (Zhang et al., 2007). In our study, the PN/PS ratio of all 4 PBRs had many changes over different periods. At days 165th, 172nd of stage 3, corresponding to the time of AAG appearance at R160, R200, the PN, PS, EPS and PN/PS values of these 2 PBRs were approximately the same and ranged from 30–35, 6.58–6.62, 36.6–41.2 mg/g biomass and 4.6–5.2, respectively. While at R120, these values of PN, PS, EPS and PN/PS were significantly different, at 58.16, 29.9, 88.1 mg/g biomass, and 1.9, respectively. These results showed two different granulation trends between the higher (R160, R200) and the lower agitation speeds (R120). Specifically, high shear stress at R160, R200 caused microorganisms to secrete a sufficient number of EPS, including PS and PN, while lower shear stress at 120 rpm required almost twice number of EPS and PN, and 5 times more PS to create AAG. This demonstrated that if there was not enough shear stress as a physical stress to help AA obtain a granular shape structure, EPS would be a compensating factor to increase the degree of particle cohesion.

In general, the biological functions of PS include energy storage and structural maintenance. In AA granulation process, it was observed that PS could be a compensatory shear stress factor for AAG formation at R120. Since PS is considered as a glue-gel compound that helps to bind and fix the structure inside the AAG, at lower shear stress (R120), the high secretion of PS indicated that when shear stress had not reached the tolerance threshold, microorganisms themselves will secrete glue-gel compound from the inside, helping them to self-isolate from the external environment and form the AAG structure. However, this EPS compensation cannot completely replace the physical stress from shear stress, as evidenced by AAG not being induced at 80 rpm even though the secreted EPS at this PBR was consistently high at $>$ 40 mg/g biomass (usually in the range of 80–100 mg/g biomass). AA at R80 could not be tightly structured and grow even though their mean diameter was the smallest of all 4 agitation speeds, since shear stress was not enough to cause the flocs to clump together to form a compact round shape like AAG at the remaining 3 speeds.

In spite of different value ranges, the microbial communities of both agitation speed thresholds still showed that AAG was formed when more PN was generated than PS, indicating that the hydrophobicity at the outer surface of AAG was a key factor in the formation

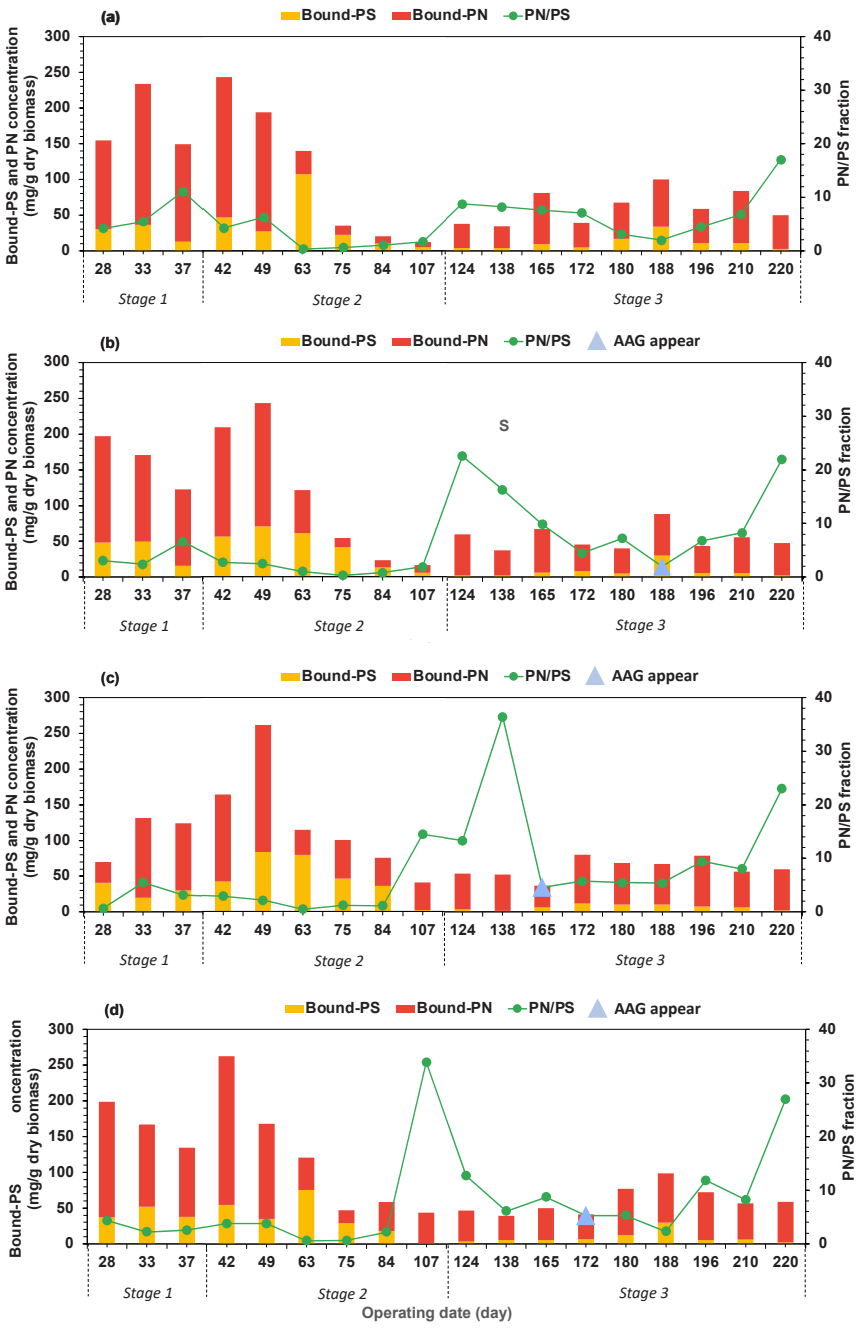




(caption on next page)

**Fig. 4.** EPS distribution over 3 stages of operation of a) R80, b) R120, c) R160, d) R200 and when e) AAG appear (for R120 – 0.15 Pa, R160 – 0.35 Pa and R200 – 0.69 Pa).

of AAG. In addition, when comparing R160 and R200 separately, the AAG size difference of these two PBRs was accompanied by a higher concentration of PN at R200, showing that when shear stress increased, the pressures generated from mechanical agitation were assumed to affect more on the outer surface of the AAG. The enhancement of PN not only increased the hydrophobicity of AAG, but it was also considered a substance that help protect the AAG structure from the outside, avoiding direct effects of higher shear stress.

### 3.6. Granulation mechanism

Right from the beginning of operation, two agitation speed thresholds of low (R80, R120) and high (R160, R200) showed a clear difference in the formation of AA, and finally in AAG. In the initial period, AA flocs from R80, R120 were in bigger size and contained more microalgae in the core than AA at R160 and R200. In addition to the layer, the AA flocs in 4 PBRs all had in common that they were made up of a core layer of filamentous microalgae, an outer layer of bacteria and microalgae *C. vulgaris* cells (Fig. 5).

According to the granulation, under the effect of shear stress, our study observed that there occurred 2 main microbial mechanisms. First was the “EPS bundles” mechanism, most pronounced in the early stages of the lower shear stress (R80, R120). When the core part began to be denser, from the core reaching the "EPS bundles" which were divided into separate arrays, including *C. vulgaris* microalgae, bacteria, "glue" substance as a substrate to connect microbial cells together (Fig. 6a). However, over time, the "EPS bundles" became vanish because with a loose structure, the suspended cell arrays will cause AA to increase the area exposed to shear stress. Receiving a lot of shear stress only caused damage to cells in the AA flocs which were relying solely on the adhesion of EPS. When these bundles were lost, the common shape of AA floc in R80 was a long rod, with many hairs sticking out around the outer layer of the floc, rather than granular shape. At the end of the experiment, microscope observation further confirmed that the AAG of R200 are the roundest of the three AAG-contained PBRs due to the highest shear stress of 0.69 Pa.

The second mechanism occurred during the granulation process of AA was “nesting effect”, which only happened under the higher shear stress condition of R160 and R200 and the later stage of R120. This effect could be clearly observed by help forming the backbone of the AAG. Microalgae can be unicellular, or grow in filaments or colonies comprised of multiple cells. Among them, growing in filaments or chains likely increases shear sensitivity relative to other microalgae due to a decrease in cell viability upon filament breakage (Wang et al., 2018). However, a different phenomena has been observed in our study, where filament is considered as backbone of AAG and being one of the two main mechanisms forming AAG. From these backbones, microalgae *C. vulgaris* will be firstly adhered, followed by bacteria cells. *C. vulgaris* (target biomass) was prioritized for inclusion in the core (Fig. 6b). Additionally, the AA flocs from these 2 PBRs in the early stages were much smaller than that of R80, R120 and did not appear to have “EPS bundles”, confirming that the formation of floating “EPS bundles” for AA to capture cells under conditions of higher shear stress was not possible. To continue increasing AA flocs size, because EPS alone was not strong enough to overcome shear stress, the mechanism of floc size growth has changed. Filamentous filaments from the core began to extend out of the EPS membrane in the border of the flocs, combined with EPS, functioned as a polymer fiber to help bind more suspended cells to increase AAG size.

AAG in the lower shear stress (R120) during stage 3 has a round shape, tight border with long and numerous filamentous microalgae. Despite the formation of AAG, the hairs produced by the filaments of the AAG at R120 did not tend to disappear but become longer. It was explained that with shear stress of 0.15 Pa, the hairs did not cause the AAG to suffer too much stress, on the contrary, increase the adhesion with other suspended cells. This phenomenon was similar to the AAG formation of R160 in stage 2. In that sense, the size of the AAG should gradually increase, but reality proved that the size of the particle in R120 can hardly grow more, because when it reached a larger size than the present, the residue tended to "separate" from the AAG, ensuring that the AAG always has a fixed range of diameter when shear stress was not high enough (Fig. 6c, d). On the other hand, this phenomena once again demonstrated that shear stress is the main factor causing the size distribution of AAG.

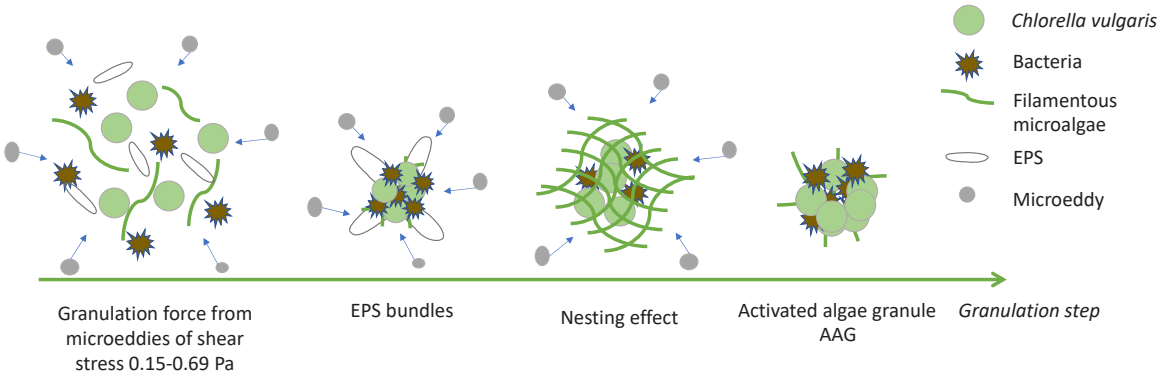


**Fig. 5.** Proposwed granulation steps of activated algae.

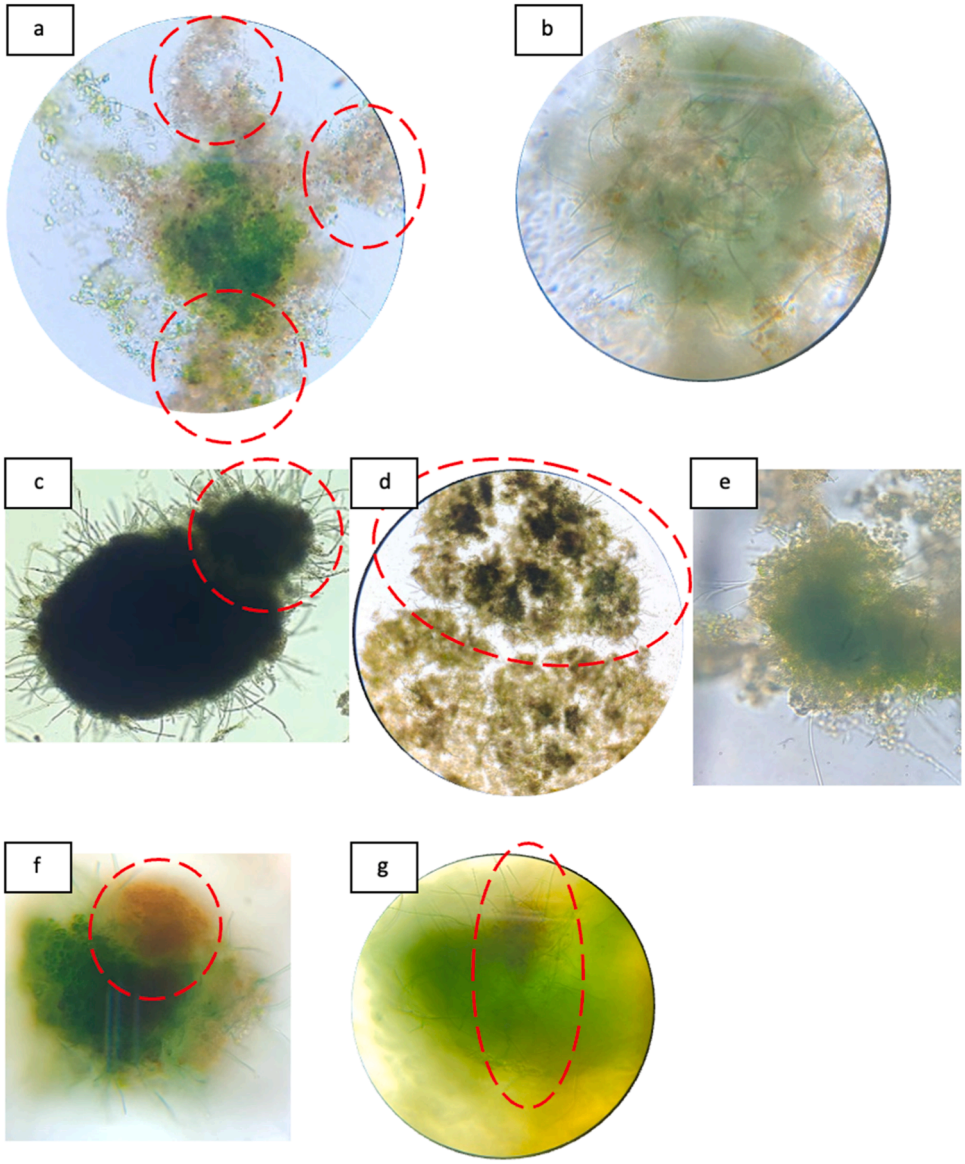


**Fig. 6.** Granulation process of AAG.

Durring granulation process, the surrounding outer layer of AA were many transparent cells with round shape like the microalgae *C. vulgaris* cells, differing only in that they were colorless, only the cell membrane was visible (Fig. 6e). Because the microalgal cells contain PN with hydrophobic amino acids, the expose of these cells to the outer layer of AA flocs showed that the microbial community tended to push the dead/colorless algal cells to outside to reinforce PN - increase hydrophobicity of the AA film, and to form the AAG.

As the microalgal cells aged and died, they tended to move out and need to be replaced by the new one, causing gaps inside the connective mass of AAG, creating cracks from the internal structure. Besides, since microalgae are autotrophs, they require $CO_2$ as a source of inorganic carbon for growth. Therefore, when located in the core of the granule, being surrounded by tight microbial layers causes a deficiency in $CO_2$ transmission. Around the outer layer of AAG were densely packed with brown bacteria flocs. Thus, through the inside granule cracks, which capture the signal from a large amount of $CO_2$ from the bacteria, an attraction between the granule core and the bacteria flocs was created to help the bacteria penetrate the AAG. In addition to the small bacteria clusters that penetrate the core of the AAG, the large ones were trapped outside, gradually combined to form larger bacterial flocs that adhere to the outside of the AAG. The agglomeration of the bacteria into large clusters created additional external pressure, causing the phenomenon that the bacteria flocs gradually penetrate the core layer of the AAG (Fig. 6f, g). The AAG structure could be changed (recessed) when the bacteria cluster tried to enter the core, but after entering the core, the AAG border was quickly restored, in order to prevent further intrusions which might cause collapse in nesting structure of AAG.

## 4. Conclusions

This is the first study to show the mechanism of granulation from activated algae without seeding granule or aeration. Activated algae granules were achieved using PBR with shear stress provided mechanically by agitation. Through this study, the mechanism of activated granule formation, and the ability of activated algae to treat wastewater during granulation process was simultaneously investigated. Over 220 days (90 batches) of operation, the results indicated that the mechanism of activated algae granule formation is mainly based on two factors, namely EPS and filamentous microalgae, which can be adjusted by agitation speed and shear stress value. The lower the shear stress the more PS was needed, the higher the shear stress the more PN was required. Particle size increase based on PN secretion. Activated algae granule was formed at 3 higher agitation speeds of 120, 160, 200 rpm with the largest particle size at R200 (339.1 μm). R160 (shear stress 0.35 Pa) gives optimal results in terms of particle formation time, as well as wastewater treatment efficiency.

## CRediT authorship contribution statement

**Ngoc-Kim-Qui Nguyen, Mai-Duy-Thong Pham:** Investigation, Software, writting original draft. **Thi-Kim-Quyen Vo, Van-Tung Tra, Thanh-Son Le:** Data curation, Conceptualization, Methodology. **Xuan-Thanh Bui, Phuoc-Dan Nguyen:** Funding, Supervision, Writting- Revieweing and Editing. **Xuan-Thanh Bui, Thanh-Son Dao, Huu Hao Ngo, Chitsan Lin, Kun-Yi Andrew Lin, Ky-Phuong-Ha Huynh**: Editing, Revise the final MS.

## Declaration of Competing Interest

The authors declare that they have no known competing financial interests or personal relationships that could have appeared to influence the work reported in this paper.

## Data Availability

No data was used for the research described in the article.

## Acknowledgements

This research is funded by Vietnam National University Ho Chi Minh City (VNU-HCM) under grant number NCM2021-20-01. In addition, the author would like to thank Mr. Hong-Hai Nguyen, Ms. Hong-Ngoc Luong, and Ms. Le-Phuong-Uyen Nguyen for their technical support. In addition, Mr. Mai-Duy-Thong Pham was funded by the Master, PhD Scholarship Programme of Vingroup Innovation Foundation (VINIF), code VINIF.2022. TS121.

## Appendix A. Supporting information

Supplementary data associated with this article can be found in the online version at doi:10.1016/j.eti.2023.103494.

## References

Abouhend, Ahmed S., Wenye, A.M., Kuo-Dahab, C., Watt, Christopher, Caitlyn, Butler, S., Milferstedt, Kim, Hamelin, J.érôme, Seo, Jeongmi, Gikonyo, Gitau J., El-MoselhyChul Park, Khalid M., 2018. The oxygenic photogranule process for aeration-free wastewater treatment. Environ. Sci. Technol. 52, 3503–3511. https://doi.org/10.1021/acs.est.8b00403.

Aditya, Lisa, Vu, Hang P., Nguyen, Luong N., Mahlia, T.M.Indra, Hoang, Ngoc Bich, Nghiem, Long D., 2023. Microalgae enrichment for biomass harvesting and water reuse by ceramic microfiltration membranes. J. Membr. Sci. 669 (2023), 121287 https://doi.org/10.1016/j.memsci.2022.121287.

Ajala, S.O., Alexander, M.L., 2022. Evaluating the effects of agitation by shaking, stirring and air sparging on growth and accumulation of biochemical compounds in microalgae cells. Biofuels 13, 371–381. https://doi.org/10.1080/17597269.2020.1714161.

Åmand, L., Olsson, G., Carlsson, B., 2013. Aeration control - a review. In: Water Science and Technology, vol. 67. IWA Publishing, pp. 2374–2398. https://doi.org/10.2166/wst.2013.139.

Ansari, Abeera A., Chul Park, A.S.A., 2019. Effects of seeding density on photogranulation and the start-up of the oxygenic photogranule process for aeration-free wastewater treatment, 101495-101495 Algal Res. 40 (April). https://doi.org/10.1016/j.algal.2019.101495.

APHA, 2005. American Water Works Association/American Public Works Association/Water Environment Federation. APHA, Washington, DC, USA. https://doi.org/10.2105/AJPH.51.6.940-a.

APHA, 2017. Standard Methods for the Examination of Water and Wastewater, 21st ed. https://doi.org/10.2105/AJPH.51.6.940-a.

Benavente-Valdés, J.R., Méndez-Zavala, A., Morales-Oyervides, L., Chisti, Y., Montañez, J., 2017. Effects of shear rate, photoautotrophy and photoheterotrophy on production of biomass and pigments by Chlorella vulgaris. J. Chem. Technol. Biotechnol. 92, 2453–2459. https://doi.org/10.1002/jctb.5256.

Bui, X.T., Fujioka, T., Nghiem, D.L., 2021. Green technologies for sustainable water (Editorial). Environ. Technol. Innov. 21, 101192 https://doi.org/10.1016/j.eti.2020.101192.

Bui, X.T., Vo, T.D.H., Thao, N.P., Nguyen, V.T., Dao, T.S., Nguyen, P.D., 2020. Microplastics pollution in wastewater: characteristics, occurrence and removal technologies. Environ. Technol. Innov. 19, 101013 https://doi.org/10.1016/j.eti.2020.101013.

Chen, H., Zhou, S., Li, T., 2010. Impact of extracellular polymeric substances on the settlement ability of aerobic granular sludge. Environ. Technol. https://doi.org/10.1080/09593330.2010.482146.

Costel Bumbac, E.M., Banciu, Alina, Stoica, Catalina, Ionescu, Ioana, Badescu, Valeriu, Nita Lazar, Mihai, 2019. Identification of physical, morphological and chemical particularities of mixed microalgae - bacteria granules. Rev. De. Chim. 70 (1) https://doi.org/10.37358/rc.19.1.6898.

Dang, B.T., Bui, X.T., Nguyen, T.T., Ngo, H.H., Nghiem, L.D., Huynh, K.P.H., Vo, T.K.Q., Vo, T.D.H., Lin, C., Chen, S.S., 2022. Effect of biomass retention time on performance and fouling of a stirred membrane photobioreactor (2023). Sci. Total Environ. 864, 161047. https://doi.org/10.1016/j.scitotenv.2022.161047.

Dang, B.T., Nguyen, T.T., Ngo, H.H., Pham, M.D.T., Le, L.T., Nguyen, N.K.Q., Vo, T.D.H., Varjani, S., You, S.J., Lin, K.A., Huynh, K.P.H., Bui, X.T., 2022b. Influence of C/N ratios on treatment performance and biomass production during co-culture of microalgae and activated sludge. Sci. Total Environ. 837, 155832 https://doi.org/10.1016/J.SCITOTENV.2022.155832.

García Camacho, F., Gallardo Rodríguez, J.J., Sánchez Mirón, A., Belarbi, E.H., Chisti, Y., Molina Grima, E., 2001. Photobioreactor scale-up for a shear-sensitive dinoflagellate microalga. Process Biochem. 46 (4), 1359–5113. https://doi.org/10.1016/j.procbio.2011.01.005.

Henzler, H.J., 2000. Particle Stress in Bioreactors. In: Schügerl, K., et al. (Eds.), Influence of Stress on Cell Growth and Product Formation, Advances in Biochemical Engineering/Biotechnology, 67. Springer. https://doi.org/10.1007/3-540-47865-5_2.

Huang, W., Li, B., Zhang, C., Zhang, Z., Lei, Z., Lu, B., Zhou, B., 2015. Effect of algae growth on aerobic granulation and nutrients removal from synthetic wastewater by using sequencing batch reactors. Bioresour. Technol. 179, 187–192. https://doi.org/10.1016/j.biortech.2014.12.024.

Ifland, J.R., Preuss, H.G., Marcus, M.T., Rourke, K.M., Taylor, W.C., Wright, H.T., Sheppard, K.K., 2015. Functional foods in the treatment of processed food addiction and the metabolic syndrome. Nutraceuticals and Functional Foods in Human Health and Disease Prevention. CRC Press, pp. 43–60. https://doi.org/10.1201/b19308.

Ji, B., 2022. Towards environment-sustainable wastewater treatment and reclamation by the non-aerated microalgal-bacterial granular sludge process: recent advances and future directions. In: Science of the Total Environment, vol. 806. Elsevier B.V. https://doi.org/10.1016/j.scitotenv.2021.150707.

Ji, M.K., Kim, H.C., Sapireddy, V.R., Yun, H.S., Abou-Shanab, R.A.I., Choi, J., Lee, W., Timmes, T.C., Inamuddin, Jeon, B.H., 2013. Simultaneous nutrient removal and lipid production from pretreated piggery wastewater by Chlorella vulgaris YSW-04. Appl. Microbiol. Biotechnol. https://doi.org/10.1007/s00253-012-4097-x.

Jirout, T., Rieger, F., 2011. Impeller design for mixing of suspensions. Chem. Eng. Res. Des. 89 (7), 1144–1151. https://doi.org/10.1016/j.cherd.2010.12.005.

Kaur, P., 2020. Microalgae as Nutraceutical for Achieving Sustainable Food Solution in Future. Springer, Singapore, pp. 91–125. https://doi.org/10.1007/978-981-15-2817-0_5.

Kim Milferstedt, W.C.K.-D., Butler, Caitlyn S., Hamelin, J.érôme, Abouhend, Ahmed S., Stauch-White, Kristie, McNair, Adam, Watt, Christopher, Carbajal González, Blanca I., Dolan, Sona, Park, Chul, 2017. The importance of filamentous cyanobacteria in the development of oxygenic photogranules. Sci. Rep. 7, 17944 https://doi.org/10.1038/s41598-017-16614-9.

Leupold, M., Hindersin, S., Gust, G., Kerner, M., Hanelt, D., 2013. Influence of mixing and shear stress on Chlorella vulgaris, Scenedesmus obliquus, and Chlamydomonas reinhardtii. J. Appl. Phycol. 25 (2), 485–495. https://doi.org/10.1007/s10811-012-9882-5.

Li, Z.H., Kuba, T., Kusuda, T., 2006. The influence of starvation phase on the properties and the development of aerobic granules. Enzym. Microb. Technol. 38 (5), 670–674. https://doi.org/10.1016/j.enzmictec.2005.07.020.

Lisa, Aditya, I. M, T.M., Luong, N., Hang, Nguyen, Vu, P., Nghiem, Long D., 2022. Microalgae-bacteria consortium for wastewater treatment and biomass production. Sci. Total Environ. 838, 155871 https://doi.org/10.1016/j.scitotenv.2022.155871.

Liu, X., Sun, S., Ma, B., Zhang, C., Wan, C., Lee, D.J., 2016. Understanding of aerobic granulation enhanced by starvation in the perspective of quorum sensing. Appl. Microbiol. Biotechnol. 100 (8), 3747–3755. https://doi.org/10.1007/s00253-015-7246-1.

Liu, Y., Wang, Z.W., Qin, L., Liu, Y.Q., Tay, J.H., 2005. Selection pressure-driven aerobic granulation in a sequencing batch reactor. Appl. Microbiol. Biotechnol. 67 (1), 26–32. https://doi.org/10.1007/S00253-004-1820-2.

Mahathir, Johan Syafri, Ahmad, Z.Z., Zhang, Zhenya, Shimizu, Kazuya, Utsumi, Motoo, Lei, Zhongfang, Lee, Duu-Jong, Tay, Joo Hwa, 2019. Algal-bacterial aerobic granule based continuous-flow reactor with effluent recirculation instead of air bubbling: Stability and energy consumption analysis. Bioresour. Technol. Rep. 7 https://doi.org/10.1016/j.biteb.2019.100215.

Masojídek, J., Ranglová, K., Lakatos, G.E., Benavides, A.M.S., Torzillo, G., 2021. Variables Governing Photosynthesis and Growth in Microalgae Mass Cultures. Processes 9 (5), 820. https://doi.org/10.3390/pr9050820.

McGriff, E.C., McKinney, R.E., 1972. The removal of nutrients and organics by activated algae. Water Res. 6 (10), 1155–1164. https://doi.org/10.1016/0043-1354(72)90015-2.

Meng, F., Xi, L., Liu, D., Huang, W., Lei, Z., Zhang, Z., Huang, W., 2019. Effects of light intensity on oxygen distribution, lipid production and biological community of algal-bacterial granules in photo-sequencing batch reactors. Bioresour. Technol. 272, 473–481. https://doi.org/10.1016/j.biortech.2018.10.059.

Metcalf, Eddy. (2014). Wastewater Engineering: Treatment and Resource Recovery: vol. *5th edition*. McGraw-Hill.

Minh, T.Vu, Luong, H.P.V., Nguyen, N., Semblante, Galilee U., Hasan Johir, Md. Abu, Nghiem, Long D., 2020. A hybrid anaerobic and microalgal membrane reactor for energy and microalgal biomass production from wastewater. Environ. Technol. Innov. 19, 100834 https://doi.org/10.1016/j.eti.2020.100834.

Minh, T.Vu, N, L.N., Mofijur, M., Hasan Johir, Md. Abu, Ngo, Hao H., Mahlia, T.M.I., Nghiem, Long D., 2022. Simultaneous nutrient recovery and algal biomass production from anaerobically digested sludge centrate using a membrane photobioreactor. Bioresour. Technol. 343, 126069 https://doi.org/10.1016/j.biortech.2021.126069.

Muñoz, R., Köllner, C., Guieysse, B., 2009. Biofilm photobioreactors for the treatment of industrial wastewaters. J. Hazard. Mater. https://doi.org/10.1016/j.jhazmat.2008.03.018.

Nguyen, Luong N., Audrey, L.L., Commault, S., Emmerton, Benjamin, Ralph, Peter J., Hasan Johir, Md. Abu, Guo, Wenshan, Ngo, Hao Huu, Nghiem, Long D., 2019. Validation of a cationic polyacrylamide flocculant for the harvesting fresh and seawater microalgal biomass. Environ. Technol. Innov. 16, 100466 https://doi.org/10.1016/j.eti.2019.100466.

Nguyen, T.T., Bui, X.T., Pham, M.D., Guo, W., Ngo, H.H., 2016. Effect of Tris-(hydroxymethyl)-amino methane on microalgae biomass growth in a photobioreactor. Bioresour. Technol. 208, 1–6. https://doi.org/10.1016/j.biortech.2016.02.043.

Nguyen, T.T., Nguyen, T.T., An Binh, Q., Bui, X.T., Ngo, H.H., Vo, H.N.P., Andrew Lin, K.Y., Vo, T.D., Guo, W., Lin, C., Breider, F., 2020. Co-culture of microalgae-activated sludge for wastewater treatment and biomass production: Exploring their role under different inoculation ratios. Bioresour. Technol. 314, 123754 https://doi.org/10.1016/j.biortech.2020.123754.

William J. Oswald, A.M. ASCE, Harold B. Gotaas, M. ASCE. (1957). Photosynthesis in sewage treatment. *American Society of Civil Engineers*, 73–97. ⟨http://content-calpoly-edu.s3.amazonaws.com/ceenve/1/images/57_photosynthesis_in_sewage_treatment.pdf⟩.

Qiulai He, L.C., Zhang, Shujia, Chen, Rongfan, Wang, Hongyu, Zhang, Wei, Song, Jianyang, 2018. Natural sunlight induced rapid formation of water-born algal-bacterial granules in an aerobic bacterial granular photo-sequencing batch reactor. J. Hazard. Mater. 359 (June), 222–230. https://doi.org/10.1016/j.jhazmat.2018.07.051.

Sforza, E., Simionato, E., Giacometti, G.M., Bertucco, A., Morosinotto, T., 2012. Adjusted Light and Dark Cycles Can Optimize Photosynthetic Efficiency in Algae Growing in Photobioreactors. PLOS ONE 7 (6), e38975. https://doi.org/10.1371/journal.pone.0038975.

Spolaore, P., Joannis-Cassan, C., Duran, E., Isambert, A., 2006. Commercial applications of microalgae. J. Biosci. Bioeng. 101 (2), 87–96. https://doi.org/10.1263/jbb.101.87.

Su, Y., Mennerich, A., Urban, B., 2012. Synergistic cooperation between wastewater-born algae and activated sludge for wastewater treatment: Influence of algae and sludge inoculation ratios. Bioresour. Technol. 105, 67–73. https://doi.org/10.1016/j.biortech.2011.11.113.

Tay, J.H., Liu, Q.S., Liu, Y., 2001. The effects of shear force on the formation, structure and metabolism of aerobic granules. Appl. Microbiol. Biotechnol. 57 (1–2) https://doi.org/10.1007/s002530100766.

Tiron, O., Patroescu, C.B., I.V., Badescu, V.R., Postolache, C., 2015. Granular activated algae for wastewater treatment. Water Sci. Technol. 71 (6), 832–839. https://doi.org/10.2166/wst.2015.010.

Verma, R., Mehan, L., Kumar, R., Kumar, A., Srivastava, A., 2019. Computational fluid dynamic analysis of hydrodynamic shear stress generated by different impeller combinations in stirred bioreactor. Biochem. Eng. J. 151, 107312 https://doi.org/10.1016/j.bej.2019.107312.

Vo, H.N.P., Bui, X.T., Nguyen, T.T., Nguyen, D.D., Dao, T.S., Cao, N.D.T., Vo, T.K.Q., 2018. Effects of nutrient ratios and carbon dioxide bio-sequestration on biomass growth of Chlorella sp. in bubble column photobioreactor. J. Environ. Manag. 219, 1–8. https://doi.org/10.1016/j.jenvman.2018.04.109.

Vo, T.K.Q., Dang, B.T., Ngo, H.H., Nguyen, T.T., Nguyen, V.T., Vo, T.D.H., Ngo, T.T.M., Nguyen, T.B., Lin, C., Lin, K.Y.A., Bui, X.T., 2021. Low flux sponge membrane bioreactor treating tannery wastewater. Environ. Technol. Innov. 24, 101989 https://doi.org/10.1016/j.eti.2021.101989.

von Alvensleben, N., Magnusson, M., Heimann, K., 2016. Salinity tolerance of four freshwater microalgal species and the effects of salinity and nutrient limitation on biochemical profiles. J. Appl. Phycol. https://doi.org/10.1007/s10811-015-0666-6.

Wang, C., Lan, C.Q., 2018. Effects of shear stress on microalgae – a review. Biotechnol. Adv. 36 (4), 986–1002. https://doi.org/10.1016/J.BIOTECHADV.2018.03.001.

Wang, L., Min, M., Li, Y., Chen, P., Chen, Y., Liu, Y., Wang, Y., Ruan, R., 2010. Cultivation of green algae Chlorella sp. in different wastewaters from municipal wastewater treatment plant. Appl. Biochem. Biotechnol. 162 (4), 1174–1186. https://doi.org/10.1007/s12010-009-8866-7.

Yao Shen, B.C., Wang, Shuo, Li, Anjie, Ji, Bin, 2023. Necessity of stirring for outdoor microalgal-bacterial granular sludge process. J. Environ. Manag. 345, 118816 https://doi.org/10.1016/j.jenvman.2023.118816.

Zhang, L., Feng, X., Zhu, N., Chen, J., 2007. Role of extracellular protein in the formation and stability of aerobic granules. Enzym. Microb. Technol. https://doi.org/10.1016/j.enzmictec.2007.05.001.

Zheng, H., Wu, X., Zou, G., Zhou, T., Liu, Y., Ruan, R., 2019. Cultivation of Chlorella vulgaris in manure-free piggery wastewater with high-strength ammonium for nutrients removal and biomass production: effect of ammonium concentration, carbon/nitrogen ratio and pH. Bioresour. Technol. 273, 203–211. https://doi.org/10.1016/j.biortech.2018.11.019.

Zhou, D., Li, Y., Yang, Y., Wang, Y., Zhang, C., Wang, D., 2015. Granulation, control of bacterial contamination, and enhanced lipid accumulation by driving nutrient starvation in coupled wastewater treatment and Chlorella regularis cultivation. Appl. Microbiol. Biotechnol. 99 (3), 1531–1541. https://doi.org/10.1007/s00253-014-6288-0.